Received: 1 April 2022 | Revised: 25 April 2022 | Accepted: 25 April 2022

DOI: 10.1111/gtc.12945

BRIEF REPORT

Genes to Cells WILEY

Luciferase-based quantification of membrane fusion induced by SARS-CoV-2 S protein

Kei Haga | **Reiko Takai-Todaka** | **Akihito Sawada** | **Kazuhiko Katayama**

Laboratory of Viral Infection, Department of Infection Control and Immunology, Ōmura Satoshi Memorial Institute & Graduate School of Infection Control Sciences, Kitasato University, Tokyo, Japan

Correspondence
Kazuhiko Katayama, Laboratory of Viral Infection, Department of Infection Control and Immunology, Ōmura Satoshi Memorial Institute & Graduate School of Infection Control Sciences, Kitasato University, Tokyo, 108-8641, Japan.
Email: katayama@lisci.kitasato-u.ac.jp

Funding information
Japan Agency for Medical Research and Development, Grant/Award Number: 21ae0121001

Communicated by: Atsushi Miyawaki

Abstract

The ongoing COVID-19 pandemic is caused by SARS-CoV-2. Although several effective vaccines that target the Spike protein on the viral surface have been deployed, additional therapeutic agents are urgently needed. Here, we developed a system to measure the Spike protein function by quantifying cellular membrane fusion induced by the Spike protein. The system enables the evaluation of the effects of drugs and neutralizing antibodies against SARS-CoV-2 without using live viruses. Furthermore, the system characterizes membrane fusion activity of the Spike protein of each variant to reveal that Delta variant has more potent than Wuhan and Omicron. Our system could lead to develop high-throughput screening for drug candidates and neutralization antibodies that target virus entry and characterize Spike proteins from variants.

1 | INTRODUCTION

SARS-CoV-2, the cause of the coronavirus disease 2019 (COVID-19) pandemic, is a betacoronavirus, and infection results in severe respiratory syndrome and sometimes death. Spike (S) proteins expressed on the envelope are required for entering the host cells. The S protein comprises two distinct parts, S1 and S2, and the receptor-binding domain (RBD) in S1 binds to the host receptor molecule, angiotensin-converting enzyme 2 (ACE2). The S protein is cleaved at the boundary of the S1 and S2 subunits, called S1/S2, but the two still bind each other non-covalently. After binding to ACE2, the conformation of the S protein is changed, and S2' site located at just upstream of fusion peptide is cleaved. This cleavage at S2' sheds the S1 subunit and induces further conformational changes to expose the fusion peptide, which fuses the viral and cellular membranes for entry. Furin protease cleaves S1/S2 site but is not essential for cell–cell fusion, while the transmembrane serine protease, TMPRSS2, has important role to form syncytium with S protein (Papa et al., 2021).

Vero E6 cells are frequently used to screen drugs and evaluate SARS-CoV-2 (Gordon et al., 2020; Jeon et al., 2020; Park et al., 2021; Shionoya et al., 2021), and TMPRSS2 transduction enhanced their susceptibility to SARS-CoV-2 (Matsuyama et al., 2020). SARS-CoV-2 infection of Vero/TMPRSS2 cells triggers a remarkable cellular fusion, termed a syncytium, among neighboring cells. It results from the binding of the S protein that is expressed on the cell surface to ACE2 on neighboring cells, and subsequent cleaving by TMPRSS2

(Buchrieser et al., 2020). The syncytium is also observed in lungs of COVID-19 patients with pneumonia and is likely involved in pathogenesis (Bussani et al., 2020; Xu et al., 2020).

Since this cell–cell fusion is triggered by the same machinery as the virus-cell fusion, compounds preventing the cell–cell fusion will be candidates for drugs to treat virus infections. In this study, we established a luciferase-based system to quantify cell–cell fusions caused by the S protein.

2 | RESULTS AND DISCUSSION

2.1 | Quantification of membrane fusion

To quantify the cell–cell membrane fusion, we used HiBit technology (Reference Figure S1 for schematic diagram). HiBit is a small 11–amino acid peptide that binds with high affinity to a larger subunit, called LgBit, to form a complex with luciferase activity. HiBit was conjugated with C-terminal of green fluorescent protein (ZsGreen). First, we transduced HiBit and LgBit in 293 T cells and co-expression strongly enhanced luciferase activity. Single expression of LgBit also slightly enhanced luciferase activity compared to single HiBit expression or non-transfection (Figure 1a). Remarkable cell fusion was observed when Vero E6 cells expressing TMPRSS2 (Vero/TMPRSS2) were infected with SARS-CoV-2 (Figure 1b). To quantify the fusion induced by virus infection, Vero/TMPRSS2 cells expressing ZsGreen-HiBit or LgBit were co-cultured in same well before SARS-CoV-2 infection. Since single LgBit was expected to enhance some degree of luciferase activity, cell numbers of LgBit expressing were changed from about 300 cells to 20,000 cells and were co-cultured with 20,000 HiBit expressing cells. The cells infected with SARS-CoV-2 showed luciferase activity from 3.4×10^7 relative luminescence unit (RLU) to 1.0×10^6 RLU (Figure 1c). Uninfected cells also showed that the luciferase activity from 6.6×10^5 RLU to 1.0×10^3 RLU depends on numbers of LgBit-expressing cells. The largest difference by presence or absence of infection was 313 cells

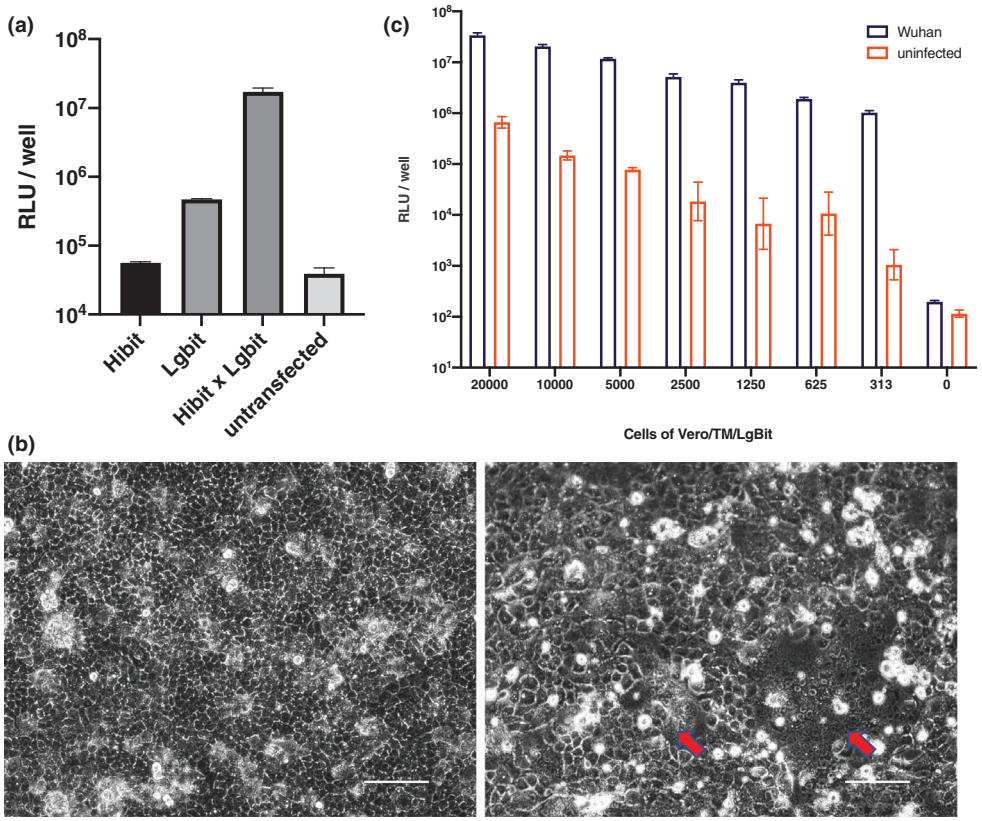

FIGURE 1 Membrane fusion assay. (a) 293 T cells were transfected ZsGreen-HiBit, LgBit, or ZsGreen-HiBit, and LgBit. At 24 hr post-transfection, cells were examined with the Nano-Glo live-cell assay system, and luciferase activity was measured. Y-axis indicates relative luminescence unit (RLU). (b) Images of Vero/TMPRSS2 cells at 24 hr post-infection with SARS-CoV-2 (left panel, uninfected cells; right panel, infected cells). Arrows indicated cellular fusion. Scale bar is 50 μm. (c) 2.0×10^4 of Vero/TMPRSS2 cells expressing Zsgreen-HiBit were co-cultured with indicated number of LgBit expressing Vero/TMPRSS2 cells (X-axis) for 24 hr. SARS-CoV-2 were infected to cells and luciferase activity was measured at 24 hr post-infection with the Nano-Glo live-cell assay system.

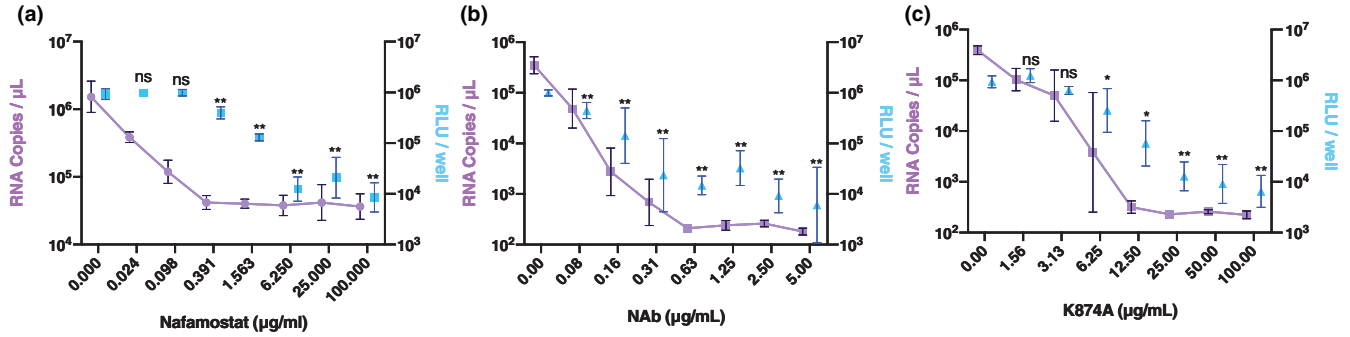

FIGURE 2 Nafamostat and neutralizing antibodies reduced cellular fusion. 2.0×10^4 of Vero/TMPRSS2 cells expressing Zsgreen-HiBit were co-cultured with 300 cells of LgBit expressing Vero/TMPRSS2 cells for 24 hr. (a) Indicated concentration of Nafamostat were treated 1 hr before infection until 24 hr post-infection. (b,c) Virus was treated indicated concentration of neutralizing antibody (b) or K-874A (c) at 37°C for 2 hr and subsequently at 4°C for overnight. Treated virus was added co-culturing cells. Treated virus was added co-culturing cells. At 24 hr post-infection, RNA copies (purple) were determined by qRT-PCR and luciferase activity (light blue) was measured with the Nano-Glo live-cell assay system. Left Y-axis indicates RNA copies and right Y-axis indicates RLU. ($N = 3$, *$p < .005$, **$p < .0001$, One-way ANOVA Dunnett's multiple comparisons test)

of LgBit-cells; therefore, further experiment in this study was conducted under this condition.

2.2 | Neutralizing antibodies or Nafamostat blocked membrane fusion and infection

We next sought to determine if HiBit-LgBit system could be used to screen anti-viral drugs targeting viral entry. First, we treated the cells with protease inhibitor, Nafamostat, which inhibits TMPRSS2 and blocks SARS-CoV-2 infection (Hoffmann et al., 2020). SARS-CoV-2 progeny was dose dependently reduced by pre-treating the cells with Nafamostat before infection (Figure 2a). Additionally, the luciferase activity was also reduced in cells treated with higher concentration of Nafamostat. To confirm, the membrane fusion was caused by S Protein, and S protein was transduced into Vero/TMPRSS2 cells by lentivirus vector. After S protein transduction into HiBit-LgBit co-culture cells, Nafamostat, likewise, inhibited luciferase activation (Figure S2). These data showed that inhibition of SARS-CoV-2 infection by Nafamostat was caused by repressing fusion between virus and cellular membrane via S protein and our cell fusion quantification system could assess S protein-induced cellular fusion.

Similarly, we tested this system using a serum from a COVID-19 convalescent patient. The 50% neutralization titer (NT_{50}) of this serum was determined ($NT_{50} = 512$) by neutralizing SARS-CoV-2. In our HiBit-LgBit system, the neutralization serum also inhibited S protein-induced cellular fusion (Figure S3). A monoclonal antibody that neutralizes SARS-CoV-2 by targeting to the receptor binding domain (RBD) of S protein also inhibited viral infection and the luciferase activation induced by cellular fusion (Figure 2b). In addition, a neutralizing nanobody, K-874A, which bound to space between N-terminal domain (NTD) and RBD of S protein and did not block S-ACE2 binding (Haga et al., 2021), also showed inhibition of SARS-CoV-2 infection and concomitant luciferase activation by cellular fusion (Figure 2b). Thus, the HiBit-LgBit system may be applied to screen for drugs against SARS-CoV-2, especially those targeting viral entry and membrane fusion.

2.3 | Transduction of S protein from each variant showed different cellular fusion activity

To gain insight into S protein property of each variant, in advance, we compared progeny production and fusogenicity among variants by infecting same infection dose of each variants to co-culturing of Vero/TMPRSS2/HiBit and Vero/TMPRSS2/LgBit cells. At 24 hr post-infection, cell fusion was observed in Wuhan-infected cells, and the Delta strain induced more prominent cell fusion, while the Omicron did not induce visible cellular fusion (Figure S4a). Progeny virus of Wuhan strain was highest and reached more than 10^7 RNA copies/μl in the culture supernatant, and progeny virus of the Delta and Omicron strains was approximately 10^5–10^6 RNA copies/μl (Figure S4b). The reason why Wuhan was higher progeny production can be inferred from that the Wuhan strain in this study was repeated passage about 10 times and may be adapted our in vitro culture condition. In contrast, the Delata and Omicorn were used after doing passage 3 times. Luciferase activity of the Delta infection was significantly higher than Wuhan infection, while that of the Omicron was significantly lower than Wuhan infection (Figure S4c).

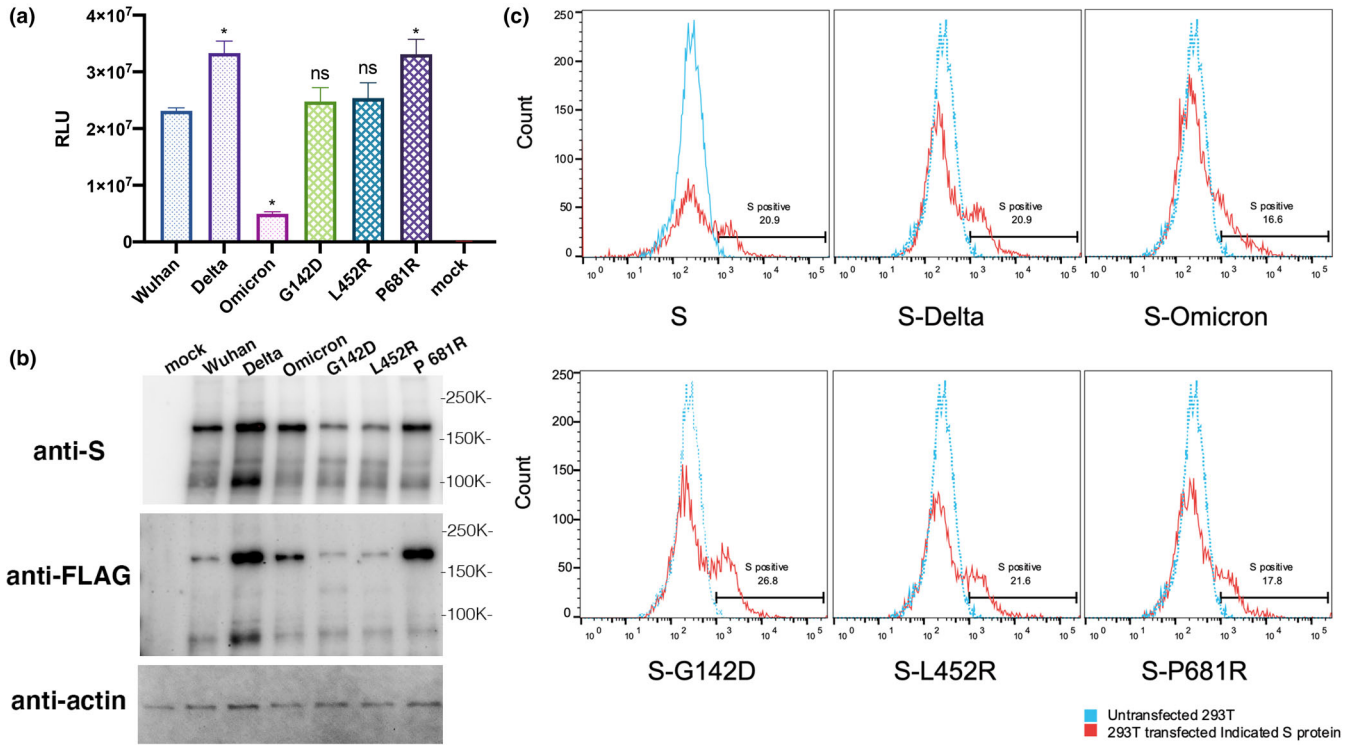

FIGURE 3 Delta S protein induces more cell fusion than the omicron strain. (a) Each FLAG-tagged S protein was transduced into 293 T cells stably expressing LgBit. At 16 hr after transduction, Vero/TMPRSS2/HiBit cells were mixed into transduced 293 T cells. After 6 hr of incubation, luciferase activity was measured with Nano-Glo live-cell assay system (*$p < .0001$, Dunnet's multiple comparison test). (b) Each transduced FLAG-tagged S protein expression in 293 T/LgBit was analyzed by western blotting using anti-S and anti-FLAG antibody. Actin was used as a loading control. (c) Each transduced FLAG-tagged S protein expression on cell surface was analyzed by flow cytometric analysis. Untransfected 293 T cells (blue line) was used as control

Since novel variants are expected to emerge one after another in the future, it is required to establish the system to evaluate promptly the antiviral effect of the developed drugs or antibodies without using live virus. Therefore, we tried to develop the system using S protein transduction instead of using live virus. We transduced S protein of each variant into 293 T cells constitutively expressing HiBit-ZsGreen and compared their fusion activity when Vero/TMPRSS2/LgBiT cells were co-cultured after S protein transduction. Cellular fusion activity of the Delta-S was higher than the Wuhan-S, while that of the Omicron-S was lower than Wuhan-S (Figure 3a). The S protein of the Delta was highly expressed in the cells compared to S protein of Wuhan and the Omicron even using the same plasmid vector to express the S proteins, while there was no difference in amount of expression on cell surface (Figure 3b,c). Three amino acid mutations were found in S protein of Delta compared to Wuhan (G142D, L452R, and P681R in NTD, RBD, and S1/S2, respectively). These mutations were individually introduced into the Wuhan-S protein. None of them impaired the expression level on the cell surface, and S-G142D and S-L452R had almost the same amount of expression and fusion ability as the Wuhan strain; however, P681R showed higher expression and fusion ability (Figure 3a–c). These data supported the recent report that P681R mutation enhanced viral fusogenicity and exhibited higher pathogenicity in infected hamsters (Saito et al., 2021). Additionally, P681R may be involved in furin protease cleavage on the S1/S2 site and enhanced infectivity (Papa et al., 2021). Our data indicated that transduction of S protein from each variant to our system reflected the nature of each S protein observed when each variant was infected to cell.

Finally, we evaluated whether neutralizing nanobody could inhibit luciferase activity of our system using S protein transduction. K-874A was treated to 293 T cells after S protein transduction. Luciferase activity was lower when 293 T cells were treated with K-874A VHH (Figure S5); however, the difference was smaller compared to using live virus. Although further optimization is required in the live-virus-free system, our system presented here can be used to screen for drugs and antibodies that impede S protein activity.

3 | EXPERIMENTAL PROCEDURES

3.1 | Cell and virus

Vero E6/TMPRSS2 cells were purchased from the JCRB Cell Bank. 293 T cells were purchased from ATCC. 293 T/

ACE2 cells were established by transducing lentiviral vector. Vero/TMPRSS2 cells were cultured in DMEM (Nacalai) with 5% FBS, Penicillin-Streptmycin (GIBCO) and 1 mg/ml G418 (Nacalai). 293 T cells were cultured in DMEM (Nacalai) with 5% FBS and Penicillin-Streptmycin. SARS-CoV-2, 2019-nCoV JPN/TY/ WK-521 (Wuhan), B.1.617.2 (Delta), and B.1.1.529 (Omicron) were provided from National Institute of Infectious Diseases (NIID, Japan). KUH003 (accession number LC630936) was isolated from nasal swabs of COVID-19 patients in Tokyo. KUH003 has D614G.

3.2 | Vector preparation

The coding sequence of the S protein without the ER retention signal was cloned into lentiviral vector, pLVSIN-IRES-puro. The 11–amino acid HiBit was inserted into the C-terminus of ZsGreen gene in pLVSIN-ZsGreen-IRES-Puro vector, and LgBit and ACE2 were cloned into the pLVSIN-IRES-Hyg vector, S proteins of each variant strain of SARS-CoV-2 were Flag-tagged at C-terminus and were cloned into pLVSIN-IRES-Puro vector.

3.3 | Lentivirus preparation and titration

Lentivirus preparation was as described (Haga et al., 2016). Briefly, lentivirus vectors were produced in HEK293 T cells by transfecting four plasmids (i.e., pMDLg/pRRE, pMD2.G, pRSV-Rev, and pLVSIN-IRE-puro-S-FLAG), using Polyethylenimine "Max" (Polysciences) as a transfection reagent. The culture supernatant was harvested 60 hr post-transfection and filtered with a 0.45-μm filter (Millipore) and stored at −80°C.

3.4 | Transduction of HiBit and LgBit

Vero/TMPRSS2 or 293 T cells were transduced with Zsgreen-HiBit or LgBit by a lentivirus vector. At 1 day after transduction, 2 μg/ml puromycin (GIBCO) or 200 μg/ml hygromycin (GIBCO) was used for selection.

3.5 | Cell fusion assay with SARS-CoV-2

HiBit technology (Promega) was used to quantify the cell fusion induced by the S protein. HiBit was linked to the C-terminus of ZsGreen (TAKARA) and transduced by lentivirus vector LVSIN-IRES-puro, and LgBit was transduced by lentivirus vector LVSIN-IRES-Hyg (Haga et al., 2016). Equal numbers of ZsGreen-HiBit-expressing cells and LgBit-expressing cells were plated on a 96-well white plate (1,603,101, ThermoFisher Science). S protein was transduced by lentivirus vector. At 14 hr after transduction, the culture supernatant was replaced with Opti-MEM (ThermoFisher Science), and 25 μl of diluted Nano-Glo live solution (Promega) was added into the each well. After mixing, the relative luminescence was measured by Ensight (Perkin Elmer).

3.6 | The 50%neutralization titer (NT_{50}) determination for neutralization serum

Four-fold serially diluted serum from a COVID-19 convalescent patient was mixed with 2.5×10^3 $TCID_{50}$ (50% Tissue Culture Infectious Dose) of SARS-CoV-2 and incubated for 2 hr at 37°C and then 24 hr at 4°C. After incubation, the virus-serum solution was added to Vero/TMPRSS2 cells and incubated for 4 days at 37°C. Cells were fixed with ice-cold methanol and stained with methylene blue. The serum dilution factor was determined by counting the wells showing cytopathic effect.

3.7 | Nafamostat and neutralizing serum treatment

Neutralizing sera were obtained from patients recovering from COVID-19. To neutralize the virus, 2.5×10^3 $TCID_{50}$ of virus was treated with the serum and incubated at 37°C for 2 hr and subsequently at 4°C for overnight. Cells were then inoculated with the serum-treated virus and were incubated for 24 hr until cell fusion assy.

3.8 | Nafamostat and neutralizing antibody and K-874A VHH treatment

Nafamostat was purchased from Selleck. Nafamostat treatment to cells was started 1 hr before infection and cells were incubated for 24 hr with medium containing each concentration of Nafamostat. To neutralize the virus, 2.5×10^3 $TCID_{50}$ of virus was treated with serial diluted neutralizing antibody (40592-MM57, Sino Biological) or K-874A neutralizing VHH (Haga et al., 2021) at 37°C for 2 hr and subsequently at 4°C for overnight. Cells were then inoculated with treated virus. At 24 hr post-infection, RNA copies of progeny virus in the culture supernatant were determined by qRT-PCR (SARS-CoV-2 Detection Kit, TOYOBO), according to manufacturer's protocol.

3.9 | S transduction to 293 T cells and cell fusion assay

Log-phase 293 T cells ($1–2 \times 10^4$) were plated on 96-well white plate (136,101, Thermo Fisher Scientific) 24 hr before transfection. For transfection, 100 ng of Flag-tagged S-protein- expressing plasmid (pLVSIN-IRE-puro-S-FLAG) was transduced into 293 T cells. At 16 hr post-transfection, Vero/TMPRSS2 cells expressing HiBit were cocultured for 6 hr, and luminescence was quantified using Nano-Glo live solution (Promega), according to manufacturer's instruction.

3.10 | Virus infection and quantification

Cells were plated on the 96-well plates and were cultured until confluent. The medium was changed to DMEM with 2% FBS, and virus solution with 2.5×10^3 $TCID_{50}$ was inoculated and incubated for 1 hr at 37°C. After infection, virus solution was removed, and wells were washed with DMEM/2% FBS and incubated for 24 hr with fresh DMEM/2% FBS. Culture supernatant at 0 days after infection was collected just after putting fresh medium. RNA copies in culture supernatant were measured by SARS-CoV-2 Detection Kit -N2 set- (TOYOBO), according to manufacturer's protocol.

3.11 | Western blotting

Whole-cell lysates were prepared by adding Laemmli's SDS/PAGE sample buffer after washing the cells with PBS(−) solution. The lysates were separated on 5%–20% polyacrylamide gels (ePAGEL; ATTO) and transferred onto a PVDF membrane by using Trans blot turbo (Bio-Rad). Anti–S protein (40591-T62, Sino Biological) and anti-FLAG-tag (F1804, SIGMA) were used as primary antibodies. HRP-conjugated anti-mouse IgG (7076, Cell Signaling Technology) and anti-rabbit IgG (7074, Cell Signaling Technology) were used as secondary antibodies. For actin detection, anti-actin hFAB rhodamine (Bio-Rad) was used. The ChemiDoc touch (Bio-Rad) was used to detect proteins visualized by Chemi-Lumi One Super (Nacalai) or rhodamine.

3.12 | Flow cytometric analysis

The expression of S protein was analyzed by FACS analysis. The cells were detached from plates by using enzyme-free dissociation buffer (Gibco). After fixing with 4% paraformaldehyde and blocking with Block ACE solution (WAKEN B TECH), rabbit anti-S protein polyclonal antibodies (40591-T62; Sino Biological) were reacted with the cells for 12 hr at 4°C. Then, the cells were washed and incubated with Alexa Fluor 488 goat anti-rabbit IgG (A-11008; Thermo Fisher) for 1 hr at 4°C. Afterward, the cells were washed and subjected to analysis. All staining and washing steps were carried out in ice-cold phosphate-buffered saline without magnesium and calcium salts [PBS(−)] solution. The cells were analyzed using a FACSMelody flow cytometry system (BD) and analyzed by using FlowJo software.

ACKNOWLEDGMENTS

This work was supported by the Japan Agency for Medical Research and Development (AMED) and the COVID-19 Kitasato project.

CONFLICT OF INTEREST

The authors declare no competing interests.

ORCID

Kazuhiko Katayama https://orcid.org/0000-0002-7692-1151

REFERENCES

Buchrieser, J., Dufloo, J., Hubert, M., Monel, B., Planas, D., Rajah, M. M., ... Schwartz, O. (2020). Syncytia formation by SARS-CoV-2-infected cells. *The EMBO Journal*, *39*(23), e106267. https://doi.org/10.15252/embj.2020106267

Bussani, R., Schneider, E., Zentilin, L., Collesi, C., Ali, H., Braga, L., ... Giacca, M. (2020). Persistence of viral RNA, pneumocyte syncytia and thrombosis are hallmarks of advanced COVID-19 pathology. *eBioMedicine*, *61*, 103104. https://doi.org/10.1016/j.ebiom.2020.103104

Gordon, D. E., Jang, G. M., Bouhaddou, M., Xu, J., Obernier, K., White, K. M., ... Krogan, N. J. (2020). A SARS-CoV-2 protein interaction map reveals targets for drug repurposing. *Nature*, *583*(7816), 459–468. https://doi.org/10.1038/s41586-020-2286-9

Haga, K., Fujimoto, A., Takai-Todaka, R., Miki, M., Doan, Y. H., Murakami, K., ... Katayama, K. (2016). Functional receptor molecules CD300lf and CD300ld within the CD300 family enable murine noroviruses to infect cells. *Proceedings of the National Academy of Sciences of the United States of America*, *113*(41), E6248–E6255. https://doi.org/10.1073/pnas.1605575113

Haga, K., Takai-Todaka, R., Matsumura, Y., Song, C., Takano, T., Tojo, T., ... Katayama, K. (2021). Nasal delivery of single-domain antibody improves symptoms of SARS-CoV-2 infection in an animal model. *PLoS Pathogens*, *17*(10), e1009542. https://doi.org/10.1371/journal.ppat.1009542

Hoffmann, M., Kleine-Weber, H., Schroeder, S., Krüger, N., Herrler, T., Erichsen, S., ... Pöhlmann, S. (2020). SARS-CoV-2 cell entry depends on ACE2 and TMPRSS2 and is blocked by a clinically proven protease inhibitor. *Cell*, *181*(2), 271–280.e278. https://doi.org/10.1016/j.cell.2020.02.052

Jeon, S., Ko, M., Lee, J., Choi, I., Byun, S. Y., Park, S., ... Kim, S. (2020). Identification of antiviral drug candidates against

SARS-CoV-2 from FDA-approved drugs. *Antimicrobial Agents and Chemotherapy*, *64*(7). https://doi.org/10.1128/AAC.00819-20

Matsuyama, S., Nao, N., Shirato, K., Kawase, M., Saito, S., Takayama, I., ... Takeda, M. (2020). Enhanced isolation of SARS-CoV-2 by TMPRSS2-expressing cells. *Proceedings of the National Academy of Sciences*, *117*(13), 7001–7003. https://doi.org/10.1073/pnas.2002589117

Papa, G., Mallery, D. L., Albecka, A., Welch, L. G., Cattin-Ortolá, J., Luptak, J., ... James, L. C. (2021). Furin cleavage of SARS-CoV-2 spike promotes but is not essential for infection and cell-cell fusion. *PLoS Pathogens*, *17*(1), e1009246. https://doi.org/10.1371/journal.ppat.1009246

Park, J. G., Oladunni, F. S., Chiem, K., Ye, C., Pipenbrink, M., Moran, T., ... Martinez-Sobrido, L. (2021). Rapid in vitro assays for screening neutralizing antibodies and antivirals against SARS-CoV-2. *Journal of Virological Methods*, *287*, 113995. https://doi.org/10.1016/j.jviromet.2020.113995

Saito, A., Irie, T., Suzuki, R., Maemura, T., Nasser, H., Uriu, K., ... Sato, K. (2021). Enhanced fusogenicity and pathogenicity of SARS-CoV-2 Delta P681R mutation. *Nature*, *602*, 300–306. https://doi.org/10.1038/s41586-021-04266-9

Shionoya, K., Yamasaki, M., Iwanami, S., Ito, Y., Fukushi, S., Ohashi, H., ... Watashi, K. (2021). Mefloquine, a potent anti-severe acute respiratory syndrome-related coronavirus 2 (SARS-CoV-2) drug as an entry inhibitor in vitro. *Frontiers in Microbiology*, *12*, 651403. https://doi.org/10.3389/fmicb.2021.651403

Xu, Z., Shi, L., Wang, Y., Zhang, J., Huang, L., Zhang, C., ... Wang, F.-S. (2020). Pathological findings of COVID-19 associated with acute respiratory distress syndrome. *The Lancet Respiratory Medicine*, *8*(4), 420–422.

SUPPORTING INFORMATION

Additional supporting information may be found in the online version of the article at the publisher's website.

How to cite this article: Haga, K., Takai-Todaka, R., Sawada, A., & Katayama, K. (2022). Luciferase-based quantification of membrane fusion induced by SARS-CoV-2 S protein. *Genes to Cells*, 1–7. https://doi.org/10.1111/gtc.12945